

Structure of the p300 Histone Acetyltransferase Bound to Acetyl-Coenzyme A and Its Analogs

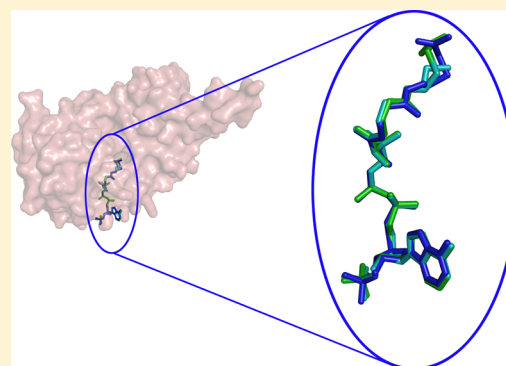
Jasna Maksimoska,^{†,‡} Dario Segura-Peña,^{†,||} Philip A. Cole,[§] and Ronen Marmorstein*,^{†,‡}

[†]Program in Gene Expression and Regulation, The Wistar Institute, 3601 Spruce Street, Philadelphia, Pennsylvania 19104, United States

[‡]Perelman School of Medicine, University of Pennsylvania, Philadelphia, Pennsylvania 19104, United States

[§]Department of Pharmacology and Molecular Sciences, Johns Hopkins University School of Medicine, 725 North Wolfe Street, Baltimore, Maryland 21205, United States

ABSTRACT: The p300 and CBP transcriptional coactivator paralogs (p300/CBP) regulate a variety of different cellular pathways, in part, by acetylating histones and more than 70 non-histone protein substrates. Mutation, chromosomal translocation, or other aberrant activities of p300/CBP are linked to many different diseases, including cancer. Because of its pleiotropic biological roles and connection to disease, it is important to understand the mechanism of acetyl transfer by p300/CBP, in part so that inhibitors can be more rationally developed. Toward this goal, a structure of p300 bound to a Lys-CoA bisubstrate HAT inhibitor has been previously elucidated, and the enzyme's catalytic mechanism has been investigated. Nonetheless, many questions underlying p300/CBP structure and mechanism remain. Here, we report a structural characterization of different reaction states in the p300 activity cycle. We present the structures of p300 in complex with an acetyl-CoA substrate, a CoA product, and an acetonyl-CoA inhibitor. A comparison of these structures with the previously reported p300/Lys-CoA complex demonstrates that the conformation of the enzyme active site depends on the interaction of the enzyme with the cofactor, and is not apparently influenced by protein substrate lysine binding. The p300/CoA crystals also contain two poly(ethylene glycol) moieties bound proximal to the cofactor binding site, implicating the path of protein substrate association. The structure of the p300/acetonyl-CoA complex explains the inhibitory and tight binding properties of the acetonyl-CoA toward p300. Together, these studies provide new insights into the molecular basis of acetylation by p300 and have implications for the rational development of new small molecule p300 inhibitors.



p300 and its CBP paralog were first described as binding partners of the adenovirus early region 1A (E1A) protein and the cAMP-regulated enhancer (CRE) binding proteins, respectively.^{1,2} It was later shown that these two highly homologous proteins, often termed p300/CBP, contribute to transcriptional regulation through their inherent histone acetyltransferase activity.^{3,4} p300 is a large protein of ~270 kDa and, in addition to its catalytic HAT region, contains several other conserved domains, including an acetyllysine binding bromodomain and zinc binding domains that directly interact with multiple cellular proteins, including many transcriptional factors.^{5,6} In addition to histones, p300 has been shown to acetylate more than 75 other substrate proteins, making it a highly promiscuous protein acetyltransferase.^{7–9} By acetylating different substrates, p300 is involved in various signaling pathways and regulates multiple cellular processes such as cell proliferation, differentiation, apoptosis, and DNA repair.¹⁰ Because of its pleiotropic roles, aberrant p300/CBP activity, through mutation, chromosomal translocation, or other p300/CBP dysregulation, has been implicated in various

diseases, including inflammation, cardiac disease, Huntington's disease, and cancer.^{10–13}

Because of the biological importance of p300/CBP and the link between aberrant p300/CBP activity and disease, there is a need to understand the mechanism of p300/CBP-mediated acetylation. Biochemical studies of p300 have revealed that the catalytic activity of the enzyme toward cognate protein substrate is regulated by p300 autoacetylation of multiple lysine residues in a proteolytically sensitive internal autoacetylation loop.^{14,15} It was shown that this intermolecular p300 acetylation is required for p300-mediated transcriptional regulation.¹⁴ The molecular basis for protein acetylation by p300 was more recently elucidated through X-ray crystallography, including the cocrystal structure of the p300 HAT domain with the synthetic bisubstrate inhibitor Lys-CoA, and the structure of the p300 catalytic core containing its bromodomain, CH2, and HAT region also in a complex with

Received: March 28, 2014

Revised: May 8, 2014

Published: May 12, 2014

Table 1. Data Collection and Refinement Statistics

	p300/acetyl-CoA	p300/CoA	p300/acetonyl-CoA
Data Collection			
space group	$P4_3$	$P4_3$	$P4_3$
cell dimensions	$a = b = 63.672 \text{ \AA}$ $c = 104.116 \text{ \AA}$ $\alpha = \beta = \gamma = 90^\circ$	$a = b = 63.672 \text{ \AA}$ $c = 104.116 \text{ \AA}$ $\alpha = \beta = \gamma = 90^\circ$	$a = b = 63.681 \text{ \AA}$ $c = 104.122 \text{ \AA}$ $\alpha = \beta = \gamma = 90^\circ$
resolution (Å)	50.00–1.94	50.00–2.10	50.00–2.80
total no. of reflections, unique	230494, 30678	83696, 24262	53041, 10279
R_{merge}^a	0.101 (0.287)	0.068 (0.359)	0.119 (0.505)
I/σ	17.3 (6.9)	18.5 (3.6)	14.8 (3.6)
completeness (%)	99.8 (98.5)	99.7 (100.0)	100.0 (100.0)
redundancy	7.5 (7.4)	3.4 (3.4)	5.2 (5.2)
Refinement			
$R_{\text{work}}/R_{\text{free}}$ (%)	18.4/23.0	16.8/21.9	15.7/23.2
Ramachandran plot (%)			
favored	96.7	96.4	97.9
allowed	2.7	3.6	2.1
disallowed	0.6 ^b	0	0
rmsd ^c for bond lengths (Å)	0.007	0.008	0.008
rmsd ^c for bond angles (deg)	1.115	1.075	1.234
B factor			
protein	26.1	40.7	38.7
ligand	23.0	37.8	32.6
solvent	31.0	43.3	31.6

^aData for the highest-resolution shell are given in parentheses. ^bRamachandran outliers: P1604 and A1605. ^cRoot-mean-square deviation.

the Lys-CoA inhibitor.^{16,17} These structures, together with related enzymatic and mutational studies, provided important insight into the catalytic mechanism of p300/CBP.¹⁶ Mutagenesis and kinetic analysis of the potential catalytic residues revealed that p300 residues Tyr1467 and Trp1436 play significant catalytic roles. On the basis of its position in the active site, we proposed that Tyr1467 played a key role in orienting the sulfur atom of acetyl-CoA and as a possible general acid by protonating the CoA leaving group.¹⁶ We also proposed that Trp1436 plays a role in orienting the cognate lysine side chain for nucleophilic attack of the acetyl-CoA cofactor.¹⁶ Taken together with the fact that p300 binds more tightly to more primitive bisubstrate analogues like Lys-CoA but much weaker to bisubstrate analogues with longer peptide chains, we proposed that p300 follows an unusual “hit-and-run” (Theorell–Chance) enzymatic mechanism.¹⁸ In this mechanism, there is no stable ternary complex formed. Instead, after acetyl-CoA binds, peptide substrate associates weakly with the p300 surface, and the target lysine then protrudes through the tunnel and reacts with the acetyl group.

Both available p300 structures are in complex with the Lys-CoA bisubstrate inhibitor, capturing a postreaction state of the enzyme. However, no structure that shows the conformation of the active site before or after the protein substrate binds is currently available. It is also not known if the protein substrate induces a conformational change upon binding that might be required for catalysis to occur. To address these issues, we determined the structures of the p300 HAT domain in the prereaction conformation in complex with acetyl-CoA, in the postreaction conformation with CoA, and in an inhibited state in complex with a nonhydrolyzable acetyl-CoA inhibitor, acetonyl-CoA. Together, the results reported in this study provide new molecular insights into p300-mediated protein acetylation and have implications for the rational development of new small molecule p300 inhibitors.

EXPERIMENTAL PROCEDURES

Protein Expression and Purification. The p300 HAT domain (residues 1279–1666, Tyr1467Phe mutation) was cloned into a pET-DUET vector with an N-terminal six-His tag and expressed in BL21(DE3) *Escherichia coli* cells. Cells were grown at 37 °C until they reached an OD₆₀₀ of 0.8, and protein expression was induced by adding 0.5 mM IPTG and cells grown overnight at 18 °C. Cells were harvested and lysed by sonication in 25 mM HEPES (pH 7.5), 500 mM NaCl, and 5 mM β-mercaptoethanol (lysis buffer). The lysate was cleared by centrifugation and applied to a Ni-NTA affinity column. The protein was eluted from the column with an increasing concentration of imidazole in lysis buffer (20–250 mM) and treated overnight with TEV protease to cleave the His₆ tag. Upon cleavage, the ligand of choice (acetyl-CoA, CoA, or acetonyl-CoA) was added to the protein solution in a 3–4-fold molar excess and incubated for 30 min to allow for binding. Protein was then subjected to a trypsin protease digest to remove the autoacetylation loop at room temperature for at least 12 h. The completeness of the digest was followed by running a protein sample on a sodium dodecyl sulfate–polyacrylamide gel electrophoresis (SDS-PAGE) gel to visualize formation of the two subdomains, the larger N-terminal subdomain (~30 kDa) and the smaller C terminal subdomain (~10 kDa). Completely digested protein was further purified by applying it on an HiTrap Q HP ion-exchange column equilibrated in 25 mM HEPES (pH 7.5), 50 mM NaCl, and 5 mM β-mercaptoethanol buffer and eluted with an increasing concentration of NaCl (from 50 to 500 mM) and a size exclusion Superdex 200 column equilibrated with 25 mM HEPES (pH 7.5), 150 mM NaCl, and 5 mM β-mercaptoethanol. The purified protein was concentrated to 6 mg/mL and used for crystallization.

Crystallization and Data Collection. Cocrystals of p300 with either CoA, acetyl-CoA, or acetonyl-CoA were obtained

using hanging drop vapor diffusion by mixing 2 μ L of a protein/ligand solution (6 mg/mL) with 1 μ L of a crystallization solution [0.1 M HEPES (pH 7.5), 16% PEG 3350, and 3–10% 2-propanol] at 4 °C. Crystals were cryoprotected in a cryosolution containing 0.1 M HEPES (pH 7.5), 18% PEG 3350, 8% 2-propanol, and 25% glycerol, flash-frozen in liquid nitrogen, and subjected to X-ray diffraction at The National Synchrotron Light Source (Brookhaven National Laboratory, Upton, NY) using beamlines X6A and X29. Collected data were integrated and scaled using HKL2000.¹⁹

Structure Determination and Refinement. Structures were determined by molecular replacement using PHASER²⁰ with the structure of the p300/Lys-CoA complex (Protein Data Bank entry 3BIY) with the Lys-CoA inhibitor removed as a search model. Model building and refinement were completed using COOT²¹ and PHENIX.²² The validity of each step of refinement and rebuilding was monitored by R_{work} and R_{free} . Data collection and refinement statistics are listed in Table 1. Structure factors and coordinates of the structures have been deposited in the Protein Data Bank as entries 4PZS (p300/acetyl-CoA), 4PZR (p300/CoA), and 4PZT (p300/acetyl-CoA).

RESULTS

Overall Structure of p300 in Complex with Acetyl-CoA. For structural studies, we focused on the p300 HAT domain, residues 1279–1666. It was previously demonstrated that the active wild-type HAT domain is toxic to bacterial cells and cannot be expressed in *E. coli*.¹⁴ Obtaining a homogeneous p300 HAT domain for crystallographic studies involved expression and purification from *E. coli* of an inactive C-terminally truncated form, reconstitution of the active intact HAT domain by semisynthetic protein ligation chemistry, proteolytic degradation to cleave the acetylation loop, and a final purification of the heterodimeric p300 HAT domain.¹⁶ To avoid this complicated and time-consuming procedure, we mutated the catalytic Tyr1467 to phenylalanine to create a catalytically inactive mutant. This allowed us to express an intact recombinant p300 HAT domain protein in *E. coli* cells in high yield (Figure 1A). Upon purification, the protein was incubated with acetyl-CoA cofactor, CoA product, or acetyl-CoA cofactor analogue and then subjected to limited proteolysis by trypsin to remove the flexible autoacetylation loop that inhibits crystallization. After trypsin digestion, two subdomains, the larger N-terminal subdomain (~30 kDa) and the smaller C-terminal subdomain (~10 kDa), formed a heterodimer that was further purified through ion-exchange and size exclusion chromatography and crystallized under similar conditions as described previously (Figure 1B).¹⁶ Our extensive efforts to obtain crystals of an intact p300 HAT domain either alone or with cofactor or cofactor analogues were unsuccessful, and limited proteolysis of p300 without added cofactor or cofactor analogues resulted in protein degradation that was not amenable to crystallization (data not shown).

The crystal structures of the p300/ligand complexes were determined by molecular replacement using the p300/Lys-CoA structure as a search model with the Lys-CoA excluded from the search model. Data collection and refinement statistics for all structures are listed in Table 1.

The overall fold of the p300 HAT domain in complex with acetyl-CoA or analogues is essentially the same as the p300 structure with Lys-CoA (Figure 2A). For example, the root-

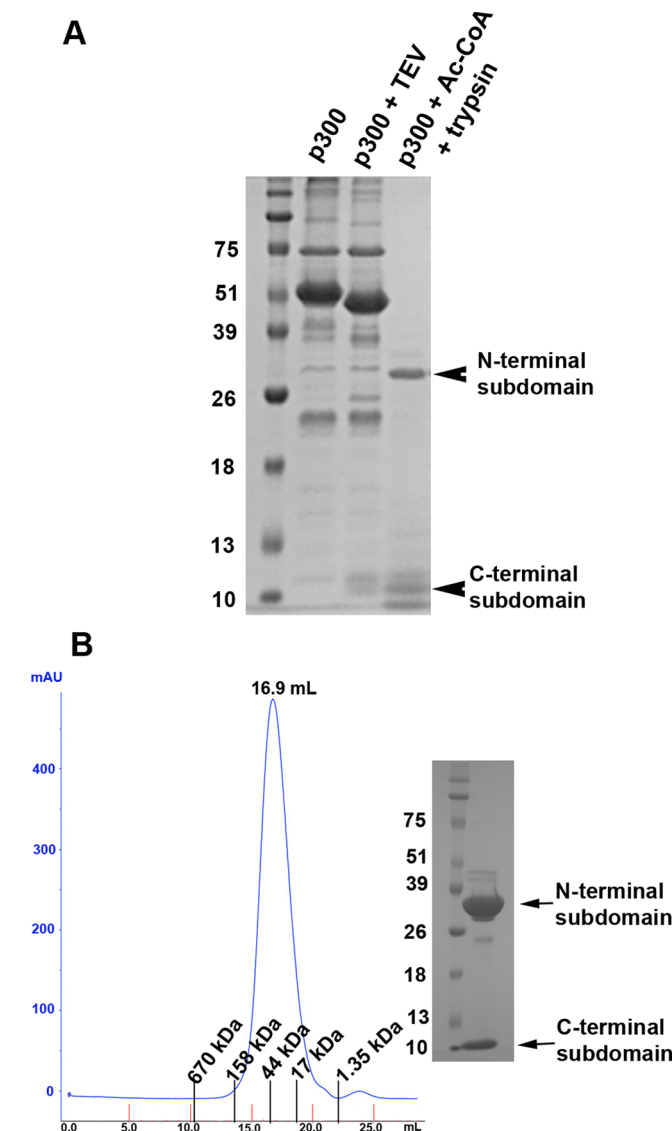


Figure 1. Expression and purification of the catalytically inactive p300 HAT domain in *E. coli* cells. (A) SDS-PAGE gel showing affinity-purified p300 HAT (first lane), the six-His tag cleavage with TEV protease (second lane), and formation of a p300 heterodimer by trypsin digestion in the presence of acetyl-CoA (third lane). Identical results of trypsin digestion were obtained in the presence of CoA and acetyl-CoA (data not shown). (B) Size exclusion chromatogram of the heterodimeric p300 HAT domain (left) and SDS-PAGE gel of the concentrated peak fractions used for crystallization (right). The elution positions of molecular weight standards are indicated.

mean-square deviation (rmsd) for all shared protein and cofactor atoms between the p300/Lys-CoA and p300/acetyl-CoA structures is 0.4 Å. The central β -sheet is composed of seven β -strands and surrounded by nine α -helices. Proteolysis of the p300 HAT domain within the autoacetylation loop prior to crystallization results in a heterodimeric HAT domain containing N- and C-terminal subdomains that are tightly associated. Trypsin digestion removes ~40 residues of the autoacetylation loop. The last residue of the N-terminal subdomain that is visible and can be modeled into the electron density map is Ser1534 (also Ser1534 for the structure with acetyl-CoA and Asn1532 for the structure with CoA), while the first residue of the C-terminal subdomain visible for all structures is Asp1579. This is in agreement with previously

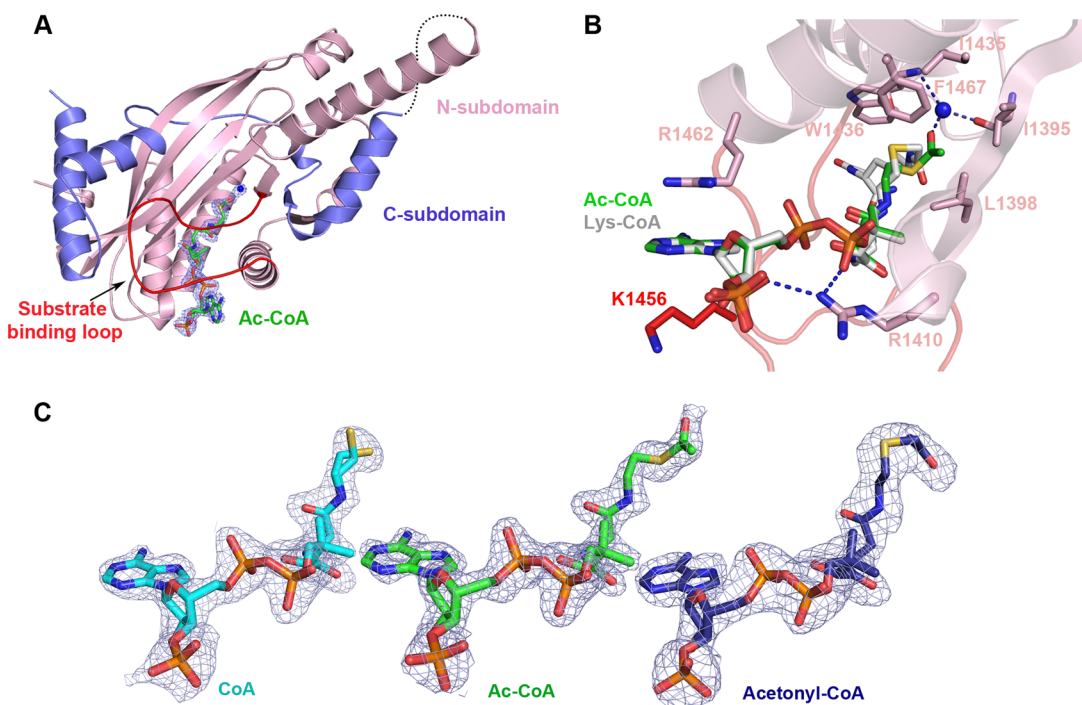


Figure 2. Overall structure of p300 in complex with acetyl-CoA. (A) Overall structure of the p300 HAT domain in complex with acetyl-CoA. Acetyl-CoA is colored green. An $F_o - F_c$ electron density map calculated before the acetyl-CoA was modeled is contoured to 2.5σ and colored blue; the N- and C-terminal subdomains are colored salmon and blue, respectively, and the substrate binding loop is colored red. The position of the proteolyzed approximately 50-residue autoacetylation loop is indicated as a dotted line. (B) Detailed view of the interactions of acetyl-CoA within the p300 binding pocket. Protein residues unique to p300 cofactor binding and coordination of a structurally conserved water molecule are labeled. Residues coming from the N-terminal subdomain are colored salmon, while Lys1456 from the substrate binding loop is colored red. Lys-CoA is shown for comparison in gray. (C) Difference $F_o - F_c$ electron density maps for CoA, Ac-CoA, and acetonyl-CoA calculated before the cofactors were modeled are colored light blue.

determined boundaries for the trypsin-digested p300 HAT domain in the presence of Lys-CoA.¹⁶ Three α -helices and one β -strand come from the smaller C subdomain, which spans the entire structure and caps opposite ends of the N subdomain. This explains the resistance to this heterodimeric portion of the HAT domain to proteolysis. The acetyl-CoA binding pocket has the same architecture as the analogous region of the Lys-CoA binding site of the p300/Lys-CoA complex. The adenine ring is sandwiched between aliphatic carbons of Arg1462 and Lys1456. Arg1410 makes several critical hydrogen bonds to phosphates, and the pantetheine arm makes extensive interactions with the substrate binding loop that closes off CoA binding in p300 (Figure 2B).

While the positions of the atoms of the terminal acetyl group of acetyl-CoA lay in the same position with their corresponding atoms of Lys-CoA (reaching toward the peptide substrate binding site), the p300/acetyl-CoA structure reveals that the acetyl group is directed toward the opposite side of the active site (Figure 2B). Difference $F_o - F_c$ electron density maps for different cofactors clearly demonstrate the difference in the position of the terminal groups in all three cofactors reported here (Figure 2C). The methyl moiety of the acetyl group is nicely accommodated by the hydrophobic residues Leu1398, Ile1395, and Ile1435. The carbonyl oxygen is coordinated to a water molecule kept in place by the backbone NH and CO groups of Trp1436 and Ile1395, respectively. Interestingly, this water molecule is conserved among the p300 structures reported here, and it likely has a role in neutralizing the negative charge that develops on the oxygen atom during the enzymatic reaction (Figure 2B). Positioned in this way, the

sulfur atom of acetyl-CoA is in a different position than it is in the Lys-CoA (or acetonyl-CoA)-containing p300 structures, such that the sulfur is 2.2 Å from the end of the Lys side chain portion of the Lys-CoA inhibitor. This position makes it ideal for nucleophilic attack by the lysine in the enzymatic reaction. In this way, the sulfur atom is still in position to be protonated by the proposed general acid, Tyr1467,¹⁶ which is replaced by the Phe mutant in this structure, after the acetyl transfer reaction occurs (Figure 2B). The cofactor sulfur atom in the wild-type and Tyr1467Phe mutant p300 HAT domain bound to the Lys-CoA inhibitor assumes the same position,^{16,17} arguing that the position of the acetyl group in acetyl-CoA is not affected by the catalytic inactivating Tyr1467Phe mutation. Taken together, we propose that the p300/acetyl-CoA complex represents the state just before the reaction occurs and the enzyme active site is ready to accept the substrate lysine.

Implications for Lysine Substrate-Mediated Structural Changes in p300. All previously reported structures of p300 are bound to the bisubstrate inhibitor Lys-CoA. Therefore, the relative contributions of the acetyl-CoA and Lys cosubstrates to the active conformation of the HAT domain are not known. A comparison of the p300 complexes with Lys-CoA, acetyl-CoA, CoA, and acetonyl-CoA reveals that the overall structures are essentially superimposable, revealing that the lysine moiety does not contribute to the formation of the active p300 HAT domain conformation (Figure 3A,B). Moreover, the conformation of the p300 HAT domain appears to be independent of the presence of additional p300 protein regions adjacent to the HAT domain because the p300 HAT domain from the recently reported p300 catalytic core structure (containing the p300

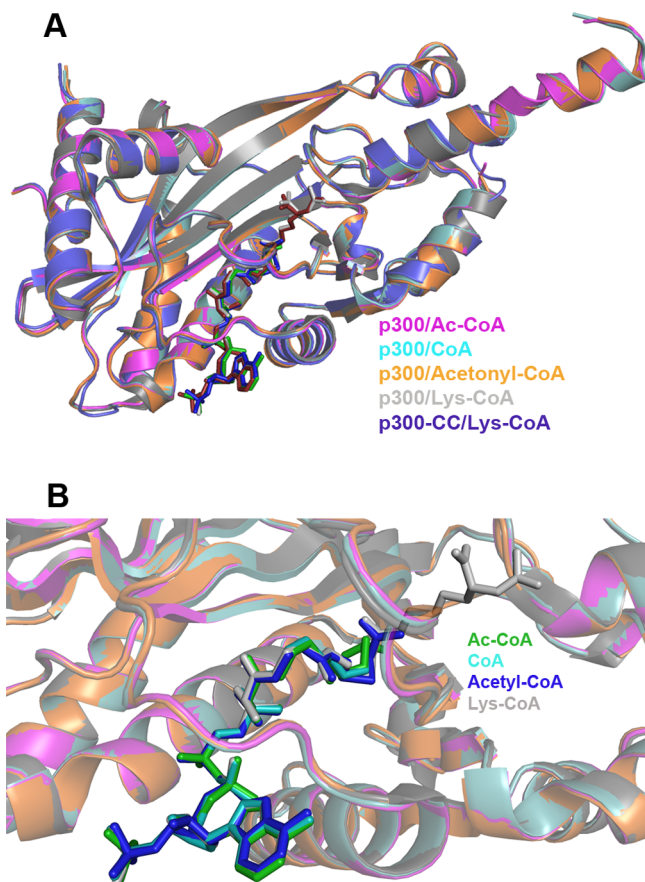


Figure 3. Comparison of the structure of p300 in complex with different ligands. (A) Superimposition of the cocrystal structures of p300 with acetyl-CoA, CoA, acetonyl-CoA, and Lys-CoA, and the HAT domain from the p300 catalytic core structure (p300-CC) illustrating a negligible degree of protein conformational change as a function of bound ligand or other adjacent domains. (B) Close-up view of the superimposed ligand binding sites.

bromo, CH₂, and HAT domains) adopts the same conformation as the structures reported here containing the isolated HAT domain¹⁷ (Figure 3A). In addition, protein residues that participate in binding of the lysine moiety of Lys-CoA adopt the same orientations in the corresponding complexes with Ac-CoA, CoA, and acetonyl-CoA. The only exception to this is residue Tyr1397. This residue is hydrogen bonded to the terminal NH group of Lys-CoA but is rotated ~60° from the enzyme active site such that Tyr1397 forms a hydrogen bond with the backbone NH group of Arg1627, a terminal residue of an α -helix. However, the relatively modest effect of a Tyr1397Phe mutation argues against the significance of this structural reorientation of Tyr1397.¹⁶ Taken together, this comparison suggests that lysine substrate binding does not contribute to the formation of the active conformation of the p300 HAT domain. This is in agreement with the proposed Theorell–Chance catalytic mechanism of p300, whereby the enzyme binds tightly to acetyl-CoA and then the lysine cosubstrate binds the enzyme with a much shorter half-life.

p300 in the Postreaction State Bound to CoA and a Pseudopeptide Substrate. To obtain molecular insight into p300 in the postreaction state, we obtained a structure of p300 bound to the CoA reaction product. The overall structure of the protein is remarkably similar to the structure of p300 bound to the acetyl-CoA substrate with an rmsd of only 0.2 Å for all

protein and all shared cofactor atoms. However, a calculated $F_o - F_c$ difference electron density map suggested that the terminal thiol group of CoA assumes two alternate conformations (Figure 2C). In one conformation, the sulfur atom assumes the same position as acetyl-CoA, while in the other conformation, the sulfur atom overlaps with the position of the sulfur atom in acetonyl-CoA and Lys-CoA (Figure 4A). The two conformations of CoA refine to relative occupancies of 60% and 40%, respectively. These alternative conformations of CoA are not surprising considering that the terminal groups of acetyl-CoA and acetonyl-CoA form interactions with the protein to help fix their orientations, and the absence of these additional interactions with CoA gives the terminal thiol group flexibility to assume different positions.

Interestingly, the refined p300/CoA structure reveals the presence of two well-ordered polyethyleneglycol (PEG) moieties, PEG1 and PEG2, presumably derived from the intact PEG polymer used for crystallization, proximal to the enzyme active site. PEG1 overlaps with the lysine moiety of the bound Lys-CoA inhibitor, and PEG2 is in an adjacent groove ~3.6 Å from PEG1 (Figure 4A).

PEG1 is within hydrogen bonding distance of the sulfur atom of one of the two orientations of the CoA molecule and is also hydrogen bonded to the backbone carbonyl group of Ser1396. The aliphatic part of PEG1 is also nicely nestled in a hydrophobic pocket formed by Trp1436, Cys1438, and the aliphatic part of Tyr1397 (Figure 4B). Notably, a corresponding PEG moiety is not observed in the p300 structures bound to acetyl-CoA or acetonyl-CoA crystallized under identical conditions. Presumably, the absence of the acetyl group and water molecule of acetyl-CoA or the acetonyl group of acetonyl-CoA allows the PEG moiety to effectively compete for this binding site in a way that mimics a lysine substrate.

PEG2 is bound right outside the lysine binding pocket, within a shallow groove formed by Arg1627 and Asp1444 (Figure 4B). PEG2 is hydrogen bonded to Arg1627, Asp1444, and the backbone carbonyl group of Asp1445, and its size fits nicely into the groove. Interestingly, because of the position of Asp1444, this groove is not accessible in the p300 structures with acetyl-CoA and acetonyl-CoA. While Arg1627 is in the same position in all structures, Asp1444 is flipped more toward Arg1627, making the groove between them much smaller and unable to accommodate PEG2 (Figure 4C).

The binding of PEG molecules near the p300 active site in the crystals is potentially interesting because it might mimic how the lysine-bearing protein substrate approaches or leaves the active site. Consistent with the path of PEG2 mimicking the path of the peptide substrate near the reactive lysine, several known histone substrates for p300 (for example, H3K14, H4K5, H4K8, and H4K12) contain one or two glycine residues or other small residues flanking the acetylated lysine that could be accommodated in this shallow groove. Many of the known non-histone p300/CBP substrates also contain glycine or alanine residues next to the primary acetylation site.^{9,16} Indeed, a characterization of the acetylation motifs of different HAT families revealed that a glycine at position –1 is the dominant residue in the three main HAT families.²³

Previous studies had identified a shallow negatively charged groove formed by residues Ser1396, Tyr1397, Thr1357, and Asp1625 on the other side of the lysine binding site as an important site for substrate binding¹⁶ (Figure 4D). We previously proposed that this negatively charged site, named P2, located approximately 10 Å from the P1 site that binds the

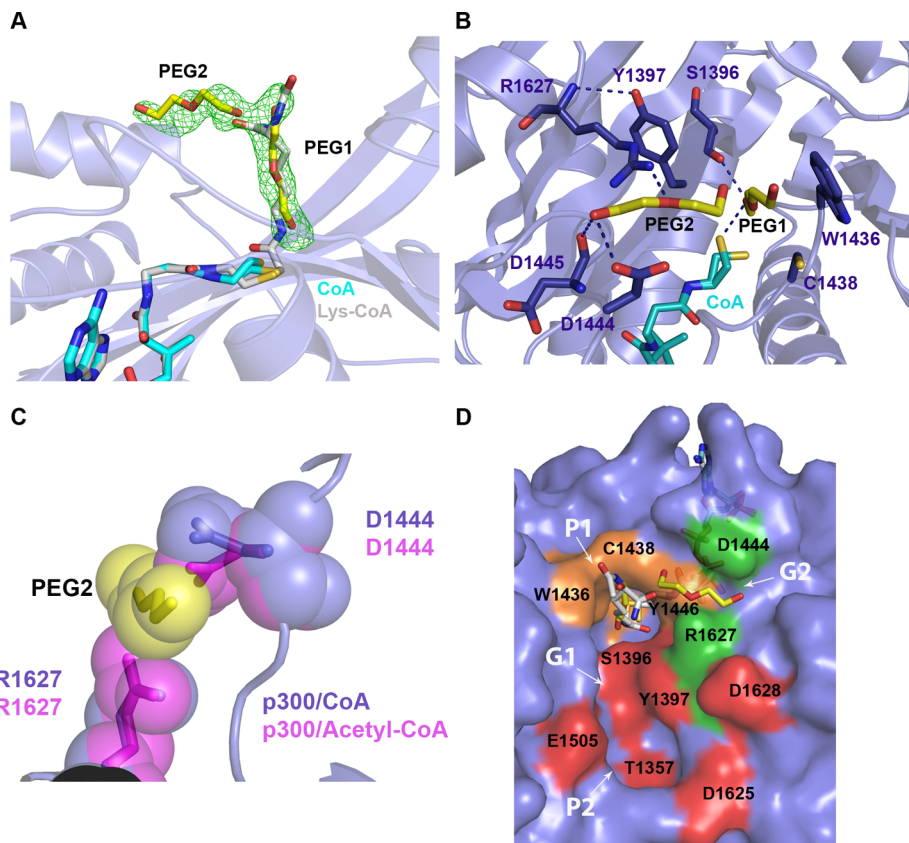


Figure 4. Structure of the p300 domain bound to CoA. (A) Superimposed active site of p300 bound to CoA and Lys-CoA. Two PEG molecules (PEG1 and PEG2) bound to the p300/CoA structure are colored yellow. An $F_o - F_c$ electron density map before the PEG molecules were modeled is contoured at 2.5σ and colored green. (B) Detailed view of the p300 active site in complex with CoA and the two bound PEG molecules. Protein residues that are important for hydrogen bonding and hydrophobic interactions with the PEG molecules are labeled. (C) van der Waals sphere representation of the PEG2 molecule and the protein residues forming the PEG binding groove. The difference in the position of the groove forming residues between the p300/CoA and p300/acetyl-CoA structures is shown. (D) Putative substrate binding surface of p300. Residues that participate in binding the substrate lysine side chain are colored orange, residues forming a negatively charged binding pocket that is proposed to contribute to substrate binding red, and residues forming a newly identified potential substrate binding groove green.

cognate lysine, could interact with a positively charged lysine or arginine side chain that is present three or four residues proximal to the cognate lysine substrate of nearly all known p300 substrates¹⁶ (Figure 4D). Taking this data together with our current observations, we propose that the path of at least a subset of p300 peptide substrates may track from PEG2 (groove 2) through the cognate lysine and toward P2 (groove 1) in either an N-terminal to C-terminal or reverse direction.

Structure of p300 Bound to the Acetonyl-CoA Inhibitor. Given the paucity of inhibitor-bound structures of p300 and other HATs, we determined the structure of p300 bound to the nonhydrolyzable acetyl-CoA analogue, acetonyl-CoA, which contains an extra methylene unit between CoA and the acetyl moiety. Given its high degree of similarity to acetyl-CoA, acetonyl-CoA has been utilized as a general inhibitor of acetyl-CoA utilizing enzymes, including HATs.²⁴ Not surprisingly, the structure of the p300/acetonyl-CoA complex superimposes almost perfectly with the p300/Lys-CoA structure with an rmsd of 0.4 Å for all protein and shared cofactor atoms. This analogous conformation likely contributes to their similar inhibitory properties. Consistent with this, both acetonyl-CoA and Lys-CoA point in opposite directions relative to the acetyl group of acetyl-CoA (Figure 5).

A more detailed analysis of the interaction of the acetonyl group with the protein shows that the acetonyl group is nicely

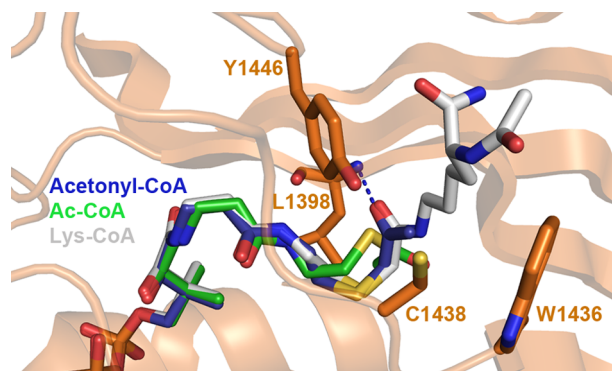


Figure 5. Structure of p300 bound to acetonyl-CoA. Superposition of acetonyl-CoA, acetyl-CoA, and Lys-CoA in the p300 binding site. For the sake of clarity, the protein is displayed only for the p300/acetonyl-CoA structure. Protein residues important for the orientation of the acetonyl group are labeled.

accommodated in the binding site, with the carbonyl hydrogen bonded to the backbone NH group of Leu1398 and the methyl group forming hydrophobic interactions with Trp1436, Cys1438, and Tyr1446 (Figure 5). These interactions that are mediated by the acetonyl group of acetonyl-CoA are consistent with the observation that acetonyl-CoA binds to

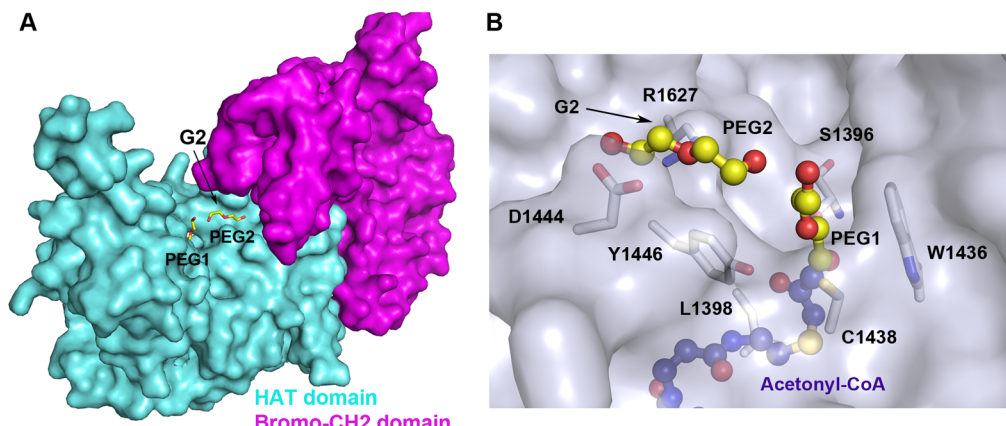


Figure 6. Superposition of the p300/CoA structure with the p300 catalytic core (with Lys-CoA) and p300/acetyl-CoA structures. (A) PEG binding site in the context of the p300 catalytic core structure, demonstrating the accessibility of the potential substrate binding site in the context of this larger p300 construct. (B) Relative positions of acetyl-CoA and PEG molecules in the p300-CoA structure are shown, demonstrating a possible target region for inhibitor development.

p300 with an affinity that is ~10-fold greater than that of CoA.¹⁶ To the best of our knowledge, the structure of the p300/acetyl-CoA complex represents the first structure of acetyl-CoA bound to a protein acetyltransferase.

■ DISCUSSION

Understanding the molecular basis for p300 acetylation is significant because of the involvement of p300 in many biological processes, the aberrant activity of p300 in many human diseases, and the implications of such studies for developing small molecule p300 inhibitors. Until now, the only p300 structures that have been reported are bound to the bisubstrate inhibitor Lys-CoA,^{16,17} and structures are notably missing for p300 bound with the acetyl-CoA substrate or CoA product, thus limiting the molecular details about the p300 reaction mechanism that could be gleaned. With this in mind, we determined the structure of p300 in complex with acetyl-CoA, CoA, and a nonhydrolyzable acetyl-CoA analogue inhibitor, acetyl-CoA.

A comparison of the structures reported here with the p300/Lys-CoA complex demonstrates that lysine substrate binding does not contribute to the active conformation of p300 and implies that acetyl-CoA binding plays a more dominant role in configuring p300 in an active conformation, consistent with the proposed Theorell–Chance catalytic mechanism.¹⁸ The p300/CoA crystals also reveal two PEG moieties bound proximal to the cofactor binding site, thus implicating a path of protein substrate association. This region of polyethylene binding to p300 remains accessible even when the adjacent p300 CH2 domain and bromodomain are present, thus likely allowing for interactions with potential protein substrates in the context of the intact p300 protein (Figure 6A).¹⁷ Given that p300 is known to acetylate more than 70 different protein substrates with somewhat diverse sequence characteristics flanking the cognate lysine residue, it is possible that p300 does not engage all substrates similarly. Therefore, the peptide path that is suggested by PEG2 may apply to only substrates that have small side chains proximal to the cognate lysine side chain.

Aside from the Lys-CoA bissubstrate p300 inhibitor,²⁵ several synthetic and natural product small molecule p300 inhibitors have been reported, including C646,²⁶ anarcardic acid,²⁷ garcinol,²⁸ curcumin,²⁹ epigallocatechin-3-gallate,³⁰ and plumbagin.³¹ Although several derivatives of many of these inhibitors

have been prepared and evaluated in cells, their biochemical analyses *in vitro* have been incomplete, and their structures with HAT proteins bound have not been determined; therefore, their mode of action is still unclear.^{32,33} The structure of the p300/acetyl-CoA and p300/CoA complexes with two PEG moieties bound proximal to the cofactor binding site provides a more rational approach to developing potent and selective small molecule p300 inhibitors. Both the acetyl group of acetyl-CoA and PEG1, which overlap the lysine binding site of p300, make stabilizing interactions with the p300 protein that may provide a starting point for a fragment-based approach for developing p300 inhibitors (Figure 6B).¹⁷ One may then be able to “grow” potency by extending the molecule into the CoA portion of the cofactor and “grow” specificity by extending the molecule into the PEG2 region or the shallow negatively charged groove that we had previously noted (Figure 4D).¹⁶ Inhibitors designed in this way may have potential as probes for the study of p300/CBP function or as therapeutic agents for the treatment of p300/CBP-mediated pathologies.

■ AUTHOR INFORMATION

Corresponding Author

*E-mail: marmor@mail.med.upenn.edu. Phone: (215) 898-7740.

Present Address

†D.S.-P.: Department of Biology, University of Pennsylvania, Philadelphia, PA 19104.

Funding

This work was supported by National Institutes of Health Grants GM062437 (to P.A.C.) and GM060293 (to R.M.).

Notes

The authors declare the following competing financial interest(s): R.M. and P.A.C. declare that they are cofounders and consultants for Acylin Therapeutics, which is developing small molecule p300 inhibitors.

■ ABBREVIATIONS

HAT, histone acetyltransferase; CoA, coenzyme A; Ac-CoA, acetyl-coenzyme A; CBP, CREB binding protein; rmsd, root mean square deviation; PEG, poly(ethylene glycol).

■ REFERENCES

- (1) Harlow, E., Whyte, P., Franzia, B. R., Jr., and Schley, C. (1986) Association of adenovirus early-region 1A proteins with cellular polypeptides. *Mol. Cell. Biol.* 6, 1579–1589.
- (2) Chirivì, J. C., Kwok, R. P., Lamb, N., Hagiwara, M., Montminy, M. R., and Goodman, R. H. (1993) Phosphorylated CREB binds specifically to the nuclear protein CBP. *Nature* 365, 855–859.
- (3) Bannister, A. J., and Kouzarides, T. (1996) The CBP co-activator is a histone acetyltransferase. *Nature* 384, 641–643.
- (4) Ogryzko, V. V., Schiltz, R. L., Russanova, V., Howard, B. H., and Nakatani, Y. (1996) The transcriptional coactivators p300 and CBP are histone acetyltransferases. *Cell* 87, 953–959.
- (5) Chen, J., Ghazawi, F. M., and Li, Q. (2010) Interplay of bromodomain and histone acetylation in the regulation of p300-dependent genes. *Epigenetics: Official Journal of the DNA Methylation Society S*, 509–515.
- (6) Kasper, L. H., Boussouar, F., Ney, P. A., Jackson, C. W., Rehg, J., van Deursen, J. M., and Brindle, P. K. (2002) A transcription-factor-binding surface of coactivator p300 is required for hematopoiesis. *Nature* 419, 738–743.
- (7) Gu, W., and Roeder, R. G. (1997) Activation of p53 sequence-specific DNA binding by acetylation of the p53 C-terminal domain. *Cell* 90, 595–606.
- (8) Yang, X. J., and Seto, E. (2008) Lysine acetylation: Codified crosstalk with other posttranslational modifications. *Mol. Cell* 31, 449–461.
- (9) Wang, L., Tang, Y., Cole, P. A., and Marmorstein, R. (2008) Structure and chemistry of the p300/CBP and Rtt109 histone acetyltransferases: Implications for histone acetyltransferase evolution and function. *Curr. Opin. Struct. Biol.* 18, 741–747.
- (10) Goodman, R. H., and Smolik, S. (2000) CBP/p300 in cell growth, transformation, and development. *Genes Dev.* 14, 1553–1577.
- (11) Shikama, N., Izuno, I., Oguchi, M., Gomi, K., Sone, S., Takei, K., Sasaki, S., Wako, T., Itou, N., and Ishii, K. (1997) Clinical stage IE primary lymphoma of the nasal cavity: Radiation therapy and chemotherapy. *Radiology* 204, 467–470.
- (12) Ogryzko, V. V., Hirai, T. H., Russanova, V. R., Barbie, D. A., and Howard, B. H. (1996) Human fibroblast commitment to a senescence-like state in response to histone deacetylase inhibitors is cell cycle dependent. *Mol. Cell. Biol.* 16, 5210–5218.
- (13) Iyer, N. G., Xian, J., Chin, S. F., Bannister, A. J., Daigo, Y., Aparicio, S., Kouzarides, T., and Caldas, C. (2007) p300 is required for orderly G1/S transition in human cancer cells. *Oncogene* 26, 21–29.
- (14) Thompson, P. R., Wang, D., Wang, L., Fulco, M., Pediconi, N., Zhang, D., An, W., Ge, Q., Roeder, R. G., Wong, J., Levrero, M., Sartorelli, V., Cotter, R. J., and Cole, P. A. (2004) Regulation of the p300 HAT domain via a novel activation loop. *Nat. Struct. Mol. Biol.* 11, 308–315.
- (15) Karanam, B., Jiang, L., Wang, L., Kelleher, N. L., and Cole, P. A. (2006) Kinetic and mass spectrometric analysis of p300 histone acetyltransferase domain autoacetylation. *J. Biol. Chem.* 281, 40292–40301.
- (16) Liu, X., Wang, L., Zhao, K., Thompson, P. R., Hwang, Y., Marmorstein, R., and Cole, P. A. (2008) The structural basis of protein acetylation by the p300/CBP transcriptional coactivator. *Nature* 451, 846–850.
- (17) Delvecchio, M., Gaucher, J., Aguilar-Gurrieri, C., Ortega, E., and Panne, D. (2013) Structure of the p300 catalytic core and implications for chromatin targeting and HAT regulation. *Nat. Struct. Mol. Biol.* 20, 1040–1046.
- (18) Segel, I. H. (1975) *Enzyme kinetics: Behavior and analysis of rapid equilibrium and steady state enzyme systems*, Wiley, New York.
- (19) Otwinowski, Z., and Minor, W. (1997) Processing of X-ray Diffraction Data Collected in Oscillation Mode. *Methods Enzymol.* 276, 307–326.
- (20) McCoy, A. J., Grosse-Kunstleve, R. W., Storoni, L. C., and Read, R. J. (2005) Likelihood-enhanced fast translation functions. *Acta Crystallogr. D61*, 458–464.
- (21) Emsley, P., and Cowtan, K. (2004) Coot: Model-building tools for molecular graphics. *Acta Crystallogr. D60*, 2126–2132.
- (22) Adams, P. D., Grosse-Kunstleve, R. W., Hung, L. W., Ioerger, T. R., McCoy, A. J., Moriarty, N. W., Read, R. J., Sacchettini, J. C., Sauter, N. K., and Terwilliger, T. C. (2002) PHENIX: Building new software for automated crystallographic structure determination. *Acta Crystallogr. S8*, 1948–1954.
- (23) Li, T., Du, Y., Wang, L., Huang, L., Li, W., Lu, M., Zhang, X., and Zhu, W. G. (2012) Characterization and prediction of lysine (K)-acetyl-transferase specific acetylation sites. *Mol. Cell. Proteomics* 11, M111.011080.
- (24) Rubenstein, P., and Dryer, R. (1980) S-acetyl-CoA. A nonreactive analog of acetyl-CoA. *J. Biol. Chem.* 255, 7858–7862.
- (25) Lau, O. D., Kundu, T. K., Soccio, R. E., Ait-Si-Ali, S., Khalil, E. M., Vassilev, A., Wolffe, A. P., Nakatani, Y., Roeder, R. G., and Cole, P. A. (2000) HATs off: Selective synthetic inhibitors of the histone acetyltransferases p300 and PCAF. *Mol. Cell* 5, 589–595.
- (26) Bowers, E. M., Yan, G., Mukherjee, C., Orry, A., Wang, L., Holbert, M. A., Crump, N. T., Hazzalin, C. A., Lisickiak, G., Yuan, H., Larocca, C., Saldanha, S. A., Abagyan, R., Sun, Y., Meyers, D. J., Marmorstein, R., Mahadevan, L. C., Alani, R. M., and Cole, P. A. (2010) Virtual ligand screening of the p300/CBP histone acetyltransferase: Identification of a selective small molecule inhibitor. *Chem. Biol.* 17, 471–482.
- (27) Sung, B., Pandey, M. K., Ahn, K. S., Yi, T., Chaturvedi, M. M., Liu, M., and Aggarwal, B. B. (2008) Anacardic acid (6-nonadecyl salicylic acid), an inhibitor of histone acetyltransferase, suppresses expression of nuclear factor- κ B-regulated gene products involved in cell survival, proliferation, invasion, and inflammation through inhibition of the inhibitory subunit of nuclear factor- κ B α kinase, leading to potentiation of apoptosis. *Blood* 111, 4880–4891.
- (28) Balasubramanyam, K., Altaf, M., Varier, R. A., Swaminathan, V., Ravindran, A., Sadhale, P. P., and Kundu, T. K. (2004) Polyisoprenylated benzophenone, garcinol, a natural histone acetyltransferase inhibitor, represses chromatin transcription and alters global gene expression. *J. Biol. Chem.* 279, 33716–33726.
- (29) Balasubramanyam, K., Varier, R. A., Altaf, M., Swaminathan, V., Siddappa, N. B., Ranga, U., and Kundu, T. K. (2004) Curcumin, a novel p300/CREB-binding protein-specific inhibitor of acetyltransferase, represses the acetylation of histone/nonhistone proteins and histone acetyltransferase-dependent chromatin transcription. *J. Biol. Chem.* 279, 51163–51171.
- (30) Choi, K. C., Jung, M. G., Lee, Y. H., Yoon, J. C., Kwon, S. H., Kang, H. B., Kim, M. J., Cha, J. H., Kim, Y. J., Jun, W. J., Lee, J. M., and Yoon, H. G. (2009) Epigallocatechin-3-gallate, a histone acetyltransferase inhibitor, inhibits EBV-induced B lymphocyte transformation via suppression of RelA acetylation. *Cancer Res.* 69, 583–592.
- (31) Ravindra, K. C., Selvi, B. R., Arif, M., Reddy, B. A., Thanuja, G. R., Agrawal, S., Pradhan, S. K., Nagashayana, N., Dasgupta, D., and Kundu, T. K. (2009) Inhibition of lysine acetyltransferase KAT3B/p300 activity by a naturally occurring hydroxynaphthoquinone, plumbagin. *J. Biol. Chem.* 284, 24453–24464.
- (32) Heery, D. M., and Fischer, P. M. (2007) Pharmacological targeting of lysine acetyltransferases in human disease: A progress report. *Drug Discovery Today* 12, 88–99.
- (33) Furdas, S. D., Kannan, S., Sippl, W., and Jung, M. (2012) Small molecule inhibitors of histone acetyltransferases as epigenetic tools and drug candidates. *Arch. Pharm. (Weinheim, Ger.)* 345, 7–21.